行政院國家科學委員會補助專題研究計畫成果報告

超音波非線性影像(II)

Ultrasonic Non-Linear Imaging (II)

計畫類別：個別型計畫
計畫編號：NSC 89-2320-B-002-152-M08
執行期間：88 年 8 月 1 日至 89 年 7 月 31 日

計畫主持人：李百祺

執行單位：台灣大學電機工程學系

中華民國 89 年 9 月 18 日

行政院國家科學委員會專題研究計畫成果報告

超音波非線性影像(II)

Ultrasonic Non-Linear Imaging (II)

計畫編號：NSC 89-2320-B-002-152-M08
執行期限：88 年 8 月 1 日至 89 年 7 月 31 日
主持人：李百祺　　台灣大學電機工程學系

一、中文摘要

由有限振幅失真所產生之第二諧波訊號會和超音波系統在發射時就加入的諧波信號混合，由於兩者頻帶相同故無法用濾波的方式加以分離，結果會造成影像品質的嚴重下降，因此必須對發射波形仔細的設計才能避免這樣的現象。

關鍵詞：超音波、非線性影像、諧波溢漏、影像品質

Abstract

Image quality degradation due to harmonic leakage was studied for finite amplitude distortion based harmonic imaging. Various sources of harmonic leakage, including transmit waveform, signal bandwidth and system nonlinearity, were investigated using both simulations and hydrophone measurements. Effects of harmonic leakage in the presence of sound velocity inhomogeneities were also considered. Results indicated that sidelobe levels of the harmonic beam pattern are directly affected by harmonic leakage. Since sidelobe levels also increase with the bandwidth of the transmitted signal, a tradeoff exists between axial resolution and contrast resolution. It is concluded that accurate control of the frequency content of the waveform prior to propagation is necessary in order to optimize imaging performance of tissue harmonic imaging.

Keywords: Ultrasound, Nonlinear Imaging, harmonic leakage, image quality.

二、緣由與目的

Finite amplitude distortion based harmonic imaging has proven to provide superior image resolution compared to conventional fundamental imaging [1]-[4]. The tissue harmonic signal is generated by nonlinearity of the propagating medium. Since the propagation velocity increases with the instantaneous acoustic pressure, the acoustic waveform is distorted during propagation and thus harmonics are generated [5]-[6]. On the other hand, harmonic signals may be generated by the imaging system itself. Such signals are independent of the nonlinear characteristics of the propagating medium. The leakage signal produces acoustic beams with different characteristics and may significantly affect image quality. It is the primary purpose of this project to investigate effects of harmonic leakage on image quality under various imaging conditions.

The block diagram of a typical ultrasound transmitter is shown in Fig. 1. A transmit waveform is produced by the

waveform generator and amplified by the high voltage amplifier. The transducer converts the electrical signal and sends out an acoustic pulse. Several sources of harmonic signals may be introduced in the transmitter. First, the signal produced by the waveform generator may have frequency components outside of the fundamental bandwidth. The amount of leakage is directly related to characteristics of the transmit waveform. In general, envelopes with a smooth shape (e.g., Gaussian envelopes) have lower harmonic amplitudes than envelopes with sharp edges (e.g., square envelopes). A wide fundamental bandwidth may also produce harmonic leakage since it may have significant overlap with the harmonic bandwidth. Second, harmonic leakage may also result from the waveform distortion produced by high voltage amplification and transmit/receive switching. Finally, the transducer may further distort the waveform during the electro-mechanical conversion. At a particular imaging depth, linear propagation of such a leakage signal is combined with the finite amplitude distortion based harmonic signal.

三、方法

Effects of various transmit waveforms on harmonic beam patterns were studied using simulations. The simulation model is similar to the one used by Christopher [1].

Simulation results shown in this report assumed a one-dimensional, 96-channel linear array. The array had a 0.25mm pitch and the transmit focus was set to 55 mm away from the transducer. The propagating medium was homogeneous. The transducer had a 3 MHz center frequency and a 80% fractional bandwidth. A displaced phase screen was included in the simulations to model sound velocity variations. Such a model is similar to the one proposed by Liu and Waag [7]. Two different media were included in the simulations. The medium next to the transducer had a propagation velocity of 1.45 mm/μs, a uniform thickness of 15 mm. The deeper medium had a propagation velocity of 1.54 mm/μs, a thickness of 65 mm. The focus was set to 55 mm away from transducer. Time delay errors resulting from irregular thickness of fat tissue were simulated using a two-dimensional phase screen at the boundary of the two media.

Hydrophone measurements were also done to experimentally investigate the harmonic leakage effects. An arbitrary function generator was used to generate the desired transmit waveform. The transmit waveform was then sent to a power amplifier to drive a 3.5 MHz focused transducer. The transducer had a diameter of 19 mm and was geometrically focused at 70 mm.

Acoustic beam patterns in water were measured by a PVDF needle hydrophone with a 30 dB pre-amplifier gain. Position of the hydrophone was controlled by a three-axis step motor system with a 5 μm step size. The signal was sent to an ultrasonic receiver for further amplification in order to match dynamic range of the analog-to-digital converter. The analog-to-digital converter had a 20 Msamples/sec sampling rate with 12-bit resolution. Acoustic beam patterns were sampled in the focal plane with a spacing of 0.1 mm. Only one-dimensional lateral measurements were performed. At each measurement point, the acoustic field was measured 1000 times for off-line signal averaging.

四、結果與討論

Simulated harmonic beam patterns of various transmit waveforms at the transmit focus are shown in Fig. 2(a). Fig. 2(b) shows the normalized, lateral integration of the intensity of the harmonic beam patterns shown in Fig. 2(a). The integration started from the center of the propagation axis and ended at a pre-specified lateral position 15mm away from the beam center. Using such a representation, a profile rises rapidly to unity represents low sidelobe levels and hence better contrast resolution. Fig. 2

demonstrates clearly that the Gaussian envelope produced significantly lower sidelobes. The two square waves had similar sidelobe levels to each other.

For a given type of waveform, the bandwidth also affects the amount of harmonic leakage. Harmonic beam patterns associated with the two bandwidths are demonstrated in Fig. 3. Similar to Fig. 2, Fig. 3(a) shows the harmonic beam patterns and Fig. 3(b) shows the normalized, laterally integrated beam patterns. It is demonstrated that the smaller bandwidth had less harmonic leakage and thus producing lower sidelobes. Although a smaller bandwidth provides lower sidelobes and better contrast resolution, one drawback is the degraded axial resolution. In other words, a tradeoff exists between axial resolution and contrast resolution.

Beam patterns produced by the Gaussian pulse, the gated sine wave and the gated square wave were simulated with sound velocity inhomogeneities. The center frequency was again 2MHz and the fractional bandwidth was 25%. Results are shown in Fig. 4. Compared to Fig. 2 (i.e., the same center frequency and bandwidth but without tissue inhomogeneities), it is observed that the tissue inhomogeneities offset a portion of contrast resolution improvement provided by the Gaussian pulse.

Effects of the signal bandwidth were also experimentally investigated. Two Gaussian pulses were used. The center frequency was 2.25 MHz for both waveforms. Bandwidths of the two waveforms were 25% and 50%. Spectra and beam patterns are demonstrated in Fig. 5 and Fig. 6 respectively. In Fig. 5, the spectra were measured near the transducer surface while the beam patterns in Fig. 6 were measured at focus. As the bandwidth increased, sidelobes were also elevated. The experimental results are consistent with previous simulations.

五、計畫成果自評

Potential degradation in contrast resolution due to harmonic leakage was investigated using both simulations and hydrophone measurements. Simulation results based on various transmit waveforms and bandwidths showed that contrast resolution in tissue harmonic imaging is directly affected by harmonic leakage. The tradeoff between contrast resolution and axial resolution was also noted. The results of this project help to better understand performance issues in tissue harmonic imaging.

六、參考文獻

[1] T. Christopher, "Finite amplitude distortion-based inhomogeneous pulse echo ultrasonic imaging," *IEEE Trans. Ultrason., Ferroelect., Freq. Contr.*, vol. 44, no. 1, pp. 125-139, Jan. 1997.

[2] T. Christopher, "Experimental investigation of finite amplitude distortion-based second harmonic pulse echo ultrasonic imaging," *IEEE Trans. Ultrason., Ferroelect., Freq. Contr.*, vol. 45, no. 1, pp. 158-162, Jan. 1998.

[3] C. A. Cain, "Ultrasonic reflection mode imaging of the nonlinear parameter B/A: I. A theoretical basis," *J. Acoust. Soc. Amer.*, vol. 80, no. 1, pp. 28-32, July 1986.

[4] R. T. Beyer and S. V. Letcher, *Nonlinear acoustics*. New York: Academic, 1969, pp. 202-230.

[5] M. E. Haran and B. D. Cook, "Distortion of finite amplitude ultrasound in lossy media," *J. Acoust. Soc. Amer.*, vol. 73, no. 3, pp. 774-779, March 1983.

[6] W. K. Law, L. A. Frizzell and F. Dunn, "Determination of the nonlinearity parameter B/A of biological media," *Ultrasound Med. Biol.*, vol. 11, no. 2, pp. 307-318, 1985.

[7] D. L. Liu and R. C. Waag, "Correction of ultrasonic wavefront distortion using backpropagation and a reference waveform method for time-shift compensation," *J. Acoust. Soc. Amer.*, vol. 96, no. 2, pp. 649-659, Aug. 1994.

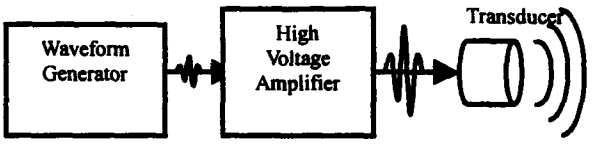

Fig. 1

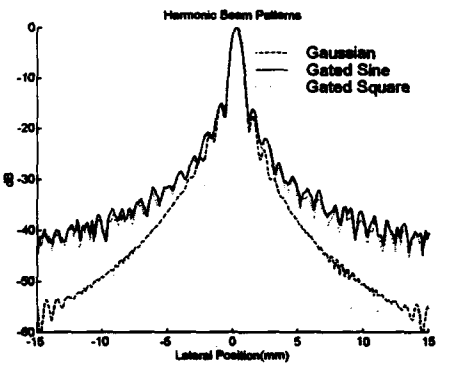

Fig. 2(a)

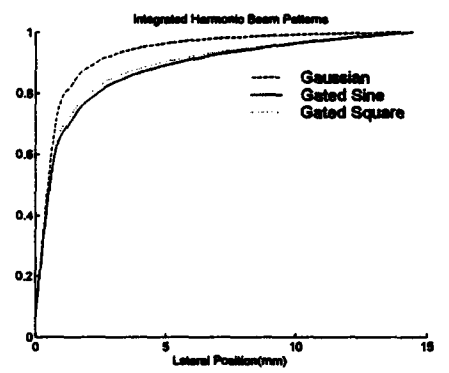

Fig. 2(b)

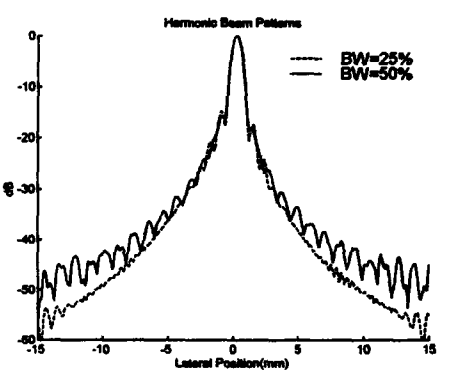

Fig. 3(a)

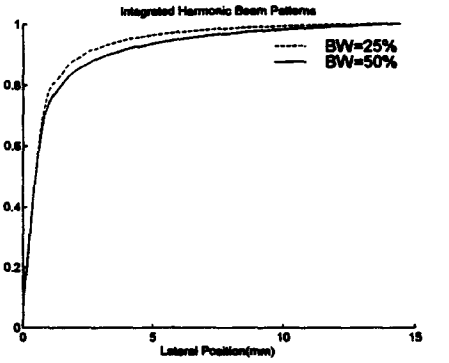

Fig. 3(b)

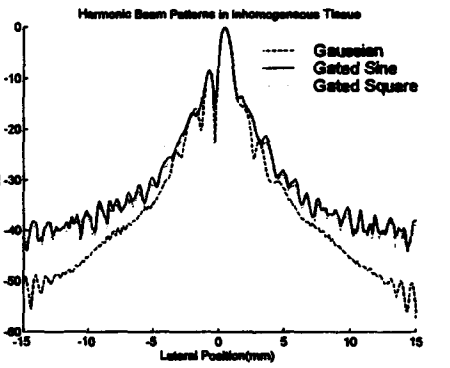

Fig. 4

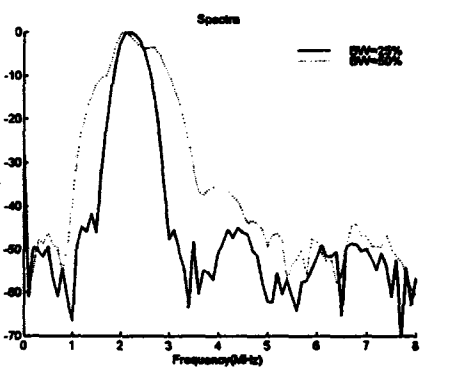

Fig. 5

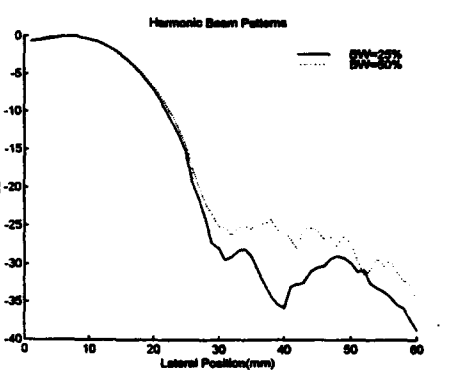

Fig. 6